

Morphologic, structural, and magnetic characterization of cobalt ferrite nanoparticles synthesized at different temperatures

Kétlin Santos Alberton

Instituto Federal de Rondônia, Campus Porto Velho Calama, Porto Velho - RO, Brasil

Liza Bruna Reis Monteiro

Instituto Federal de Rondônia, Campus Porto Velho Calama, Porto Velho - RO, Brasil

Anne Beatriz Ramos Moraes

Instituto Federal de Rondônia, Campus Porto Velho Calama, Porto Velho - RO, Brasil

Raynara Vitória dos Santos Paiva Bucar

Instituto Federal de Rondônia, Campus Porto Velho Calama, Porto Velho - RO, Brasil

Maicon Maciel Ferreira de Araújo

Instituto Federal de Rondônia, Campus Porto Velho Calama, Porto Velho - RO, Brasil

Moacy José Stoffes Junior

Instituição: Instituto Federal do Paraná, Campus Telêmaco Borba, Telêmaco Borba – PR, Brasil

E-mail: moacy.stoffes@ifpr.edu.br

Cléver Reis Stein (corresponding author)

Instituto Federal de Rondônia, Campus Porto Velho Calama, Porto Velho - RO, Brasil

E-mail: clever.stein@ifro.edu.br

Abstract

In this study we report on the synthesis and characterization of cobalt ferrite (CoFe₂O₄) nanoparticles (NPs), synthesized by chemical co-precipitation in alkaline medium. Two samples were synthesized at two different temperatures, 35 and 90 °C. Both samples were characterized by Transmission Electron Microscopy (TEM), x-ray diffraction (XRD), and room-temperature (RT) magnetization. Two samples showed superparamagnetic behavior (SPM) at RT. TEM reveals morphological mean diameter increasing 5.8 nm to 10.4 nm, with the increase of the co-precipitation temperature. XRD confirm the inverse cubic spinel structure. The RT magnetization curves were analyzed by the first-order Langevin function averaged out by a lognormal distribution function of magnetic moments. This analysis showed saturation magnetization and magnetic moment increases from 60.2 to 74.8 emu/g and from 3.9 x 10³ to 8.2 x 10³ μ_B, respectively.

Keywords: Co-precipitation; temperature; cobalt ferrite nanoparticle; hysteresis cycle.

1. Introduction

Nanosized cobalt ferrite (CoFe_2O_4) has attracted continuous interest over the past last decades due to a variety of applications it has been connected with; to name a few magneto-optical devices [1], drug delivery systems [2], contrast agent for MRI [3], magneto hyperthermia [4], and spintronics [5]. Reduced dimensionality of cobalt ferrite explains differences in properties while compared to its bulk counterpart [6,7,8]. Size modulation of the physicochemical properties of cobalt ferrite is a typical response in the nanosized regime, allowing for material engineering in order to meet different requirements while addressing applications [9]. In addition to size and size dispersity [10], material engineering regarding core-shell design [11], shape [12], crystallinity [13,14], surface decoration [15] and hybrid derivatives [16] open up a wide variety of opportunities for basic studies as well as for development and innovation. Despite different synthesis routes for nanosized cobalt ferrite already described in the literature optimization of morphology and physicochemical properties is still far from being exhausted [17,18]. In this study we report on the synthesis, structural characterization, morphological and magnetic properties of cobalt ferrite nanoparticles realized in two different temperatures.

2. Experimental

In a first step the nanosized cobalt ferrite particles were synthesized by coprecipitation in alkaline medium [19, 20, 21]. In addition to having a low cost this method of synthesis usually provides nanosized particles with relative narrow size distribution at low sintering temperatures [22,23]. In short, acidic aqueous solutions ($0.02 \text{ mol}\times\text{L}^{-1} \text{ HCl}$) containing Fe^{3+} and Co^{2+} ions were mixed in stoichiometric 2:1 ($\text{Fe}_3^+:\text{Co}_2^+$) molar ratio under stirring (200 rpm) for 20 minutes, at different temperatures (35 and 90 °C). Next, 50 mL of sodium hydroxide (NaOH) aqueous solution ($5.1 \text{ mol}\times\text{L}^{-1}$), pre-heated at the same temperature, was added into the reaction medium while keeping the same stirring speed (220 rpm) and temperature (35 and 90 °C) for another 30 minutes. The repeated synthesis protocol produced two different samples, namely CoT35, and CoT90. After synthesis, each product was naturally cooled down to room temperature and separated by magnetic decantation. The supernatant was disregarded and precipitate washed with water several times. The resulting slurries were dried at 30 °C in order to carry on morphological, structural, and magnetic characterization. The TEM micrographs were collected in a Jeol model JEM-1010 electron microscope system (Gatan Digital Micrograph) operating at 80 kV. x-ray diffraction (XRD) was used to characterize the as-synthesized samples while providing estimative of the crystallite size. XRD data of all samples were recorded in a Shimadzu model XRD 6000 system using the $\text{Cu K}\alpha$ ($\lambda = 1.5418 \text{ \AA}$) line scanning in the range of $2\theta = 10 - 80^\circ$ at 2 degrees/minute. A SQUID MPMS 3 system (Quantum Design, San Diego California - USA) was used to collect the room-temperature hysteresis cycles in the range of $\pm 60 \text{ kOe}$.

3. Results and discussion

A typical TEM micrograph of sample CoT35, and CoT90, and the corresponding particle size histogram (800 counts) are shown in Figure 1.

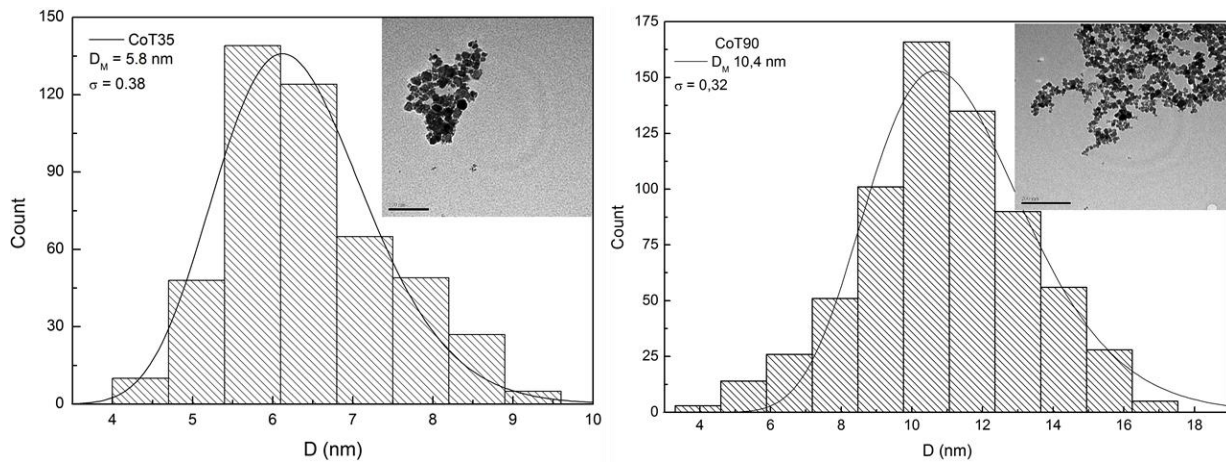


Figure 1. Particle size histogram and the curve fitting using a log-normal distribution function. The inset shows a typical TEM micrograph of samples CoT35, and CoT90.

The solid line going through the particle size histogram represents the best curve fitting using a log-normal distribution function, with σ_T and D_T collected in Table 1 and representing the standard deviation and the mean morphological diameter, respectively [18a].

$$P(D) = \frac{\exp(2\sigma_M^2)}{D_T \sigma_T \sqrt{2\pi}} \exp[\ln^2(D/D_T)/2\sigma_T^2] \quad (1)$$

Analysis of the XRD data shown in Figure 2 reveals typical features of cubic spinel (Fd-3m (227)) structure in all two produced samples and are well indexed to the cobalt ferrite spinel structure (JCPDS card No. 22-1086). Analysis of the strongest XRD reflection peak (311 reflection) using the Scherrer's relation shown below provides the average crystallite diameter [26]:

$$D_{hkl} = \frac{0.9\lambda}{\beta \cos\theta} \quad (2)$$

where D_{hkl} , λ , β and θ represent the average crystallite diameter, X-ray wavelength, full-width at half-maximum (FWHM) of probed XRD reflection peak and the Bragg's angle, respectively.

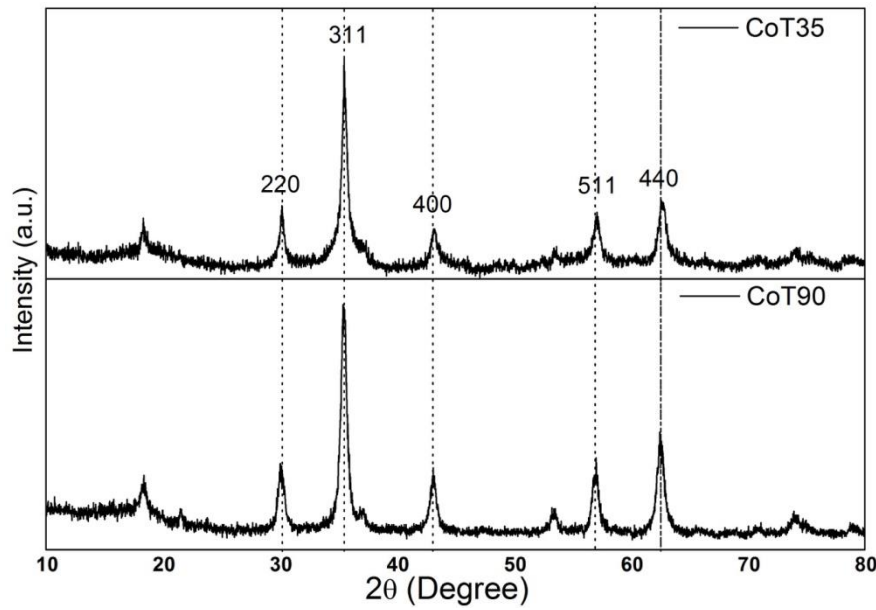


Figure 2. Diffraction pattern of cobalt ferrite nanoparticle of samples CoT35, and CoT90. The average crystallite diameters (D_{hkl}) obtained from the (311) XRD peaks of both samples are collect in Table 1.

Analysis of the room-temperature ($T = 300$ K) magnetization (M) versus applied field (H) data shown in Figure 3 (symbols) is carried over using the first-order Langevin function (L) averaged out by the lognormal distribution function (f) of particle’s magnetic moment (μ):

$$M(H, T) = M_s \int_{\mu_-}^{\mu_+} \mu L\left(\frac{\mu H}{k_B T}\right) f(\mu) d\mu \quad (3)$$

$$f(\mu) = \left(\frac{N}{\sigma_\mu \mu \sqrt{2\pi}}\right) \exp\left\{-\left[\frac{\ln^2(\mu/\mu_0)}{2\sigma_\mu^2}\right]\right\} \quad (4)$$

where N represents particle/cm³, μ_0 is the average magnetic moment, and σ_μ is the magnetic moment dispersity. Solid lines going through the symbols in Figure 3 represent the best fitting of the data using Eq. (3). The estimated values of the saturation magnetization (M_s) and average magnetic moment (μ_0) are collected in Table 1.

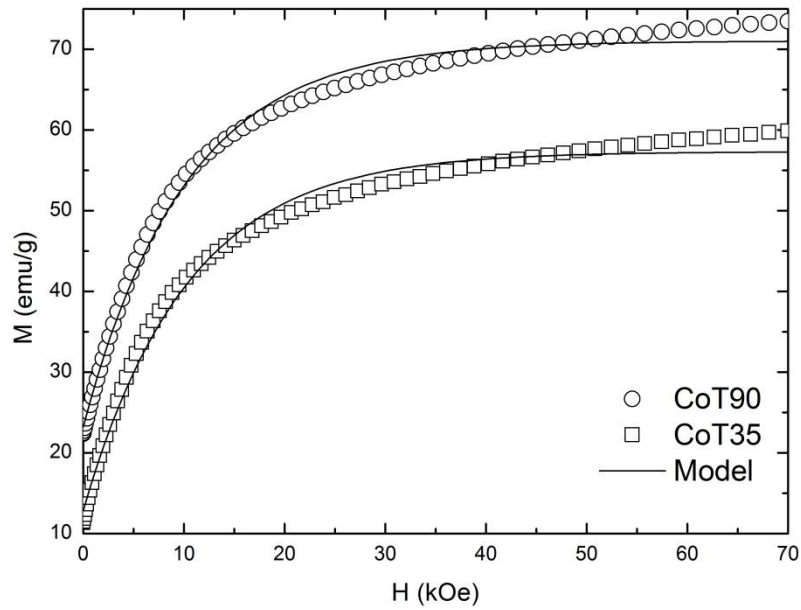


Figure 3. Magnetization loops data (symbols) of two samples (CoT35, and CoT90) and the corresponding curve fitting (solid lines) using a eq. 3.

Table 1. Mean morphological diameter D_T , standard deviation σ_T of D_T , Crystallite diameter D_{hkl} , average magnetic moment μ_0 , standard deviation σ_μ of μ_0 , and saturation magnetization M_s .

Samples	D_T (nm)	σ_T	D_{hkl} (nm)	μ_0 ($10^3 \mu_B$)	σ_μ	M_s (emu/g)
CoT35	5.8	0.38	5.4	3.9	0.47	60.2
CoT90	10.4	0.32	8.1	8.2	0.35	74.8

The same change in average diameter assessed from both TEM and XRD data while increasing synthesis temperature in the saturation magnetization values and the average magnetic moment. Moreover, as the average particle diameter increases the saturation magnetization increases monotonically. Actually, enhancement of the saturation magnetization is due to the increase of the average particle diameter and improvement in crystallization, both working to strength magnetic ordering.

4. Conclusion

In this study cobalt ferrite nanoparticles were synthesized by coprecipitation method in alkaline medium in two different temperatures. Two prepared samples were structurally, morphologically and magnetically characterized using x-ray diffraction, Transmission Electron Microscopy and room-temperature hysteresis cycle. TEM and XRD data showed that all produced samples were single-phased with diameters in the nanosized range and below 12 nm. The first-order Langevin function averaged out by the lognormal distribution function of magnetic moments provided excellent fitting of the magnetization versus magnetic field data. All results showed systematic evolution of mean diameter, as the synthesis temperature increases from 35 to 90 °C.

5. Acknowledgement

The authors thanks Brazilian agency CNPq for the financial support and Federal Institute of Rondônia-IFRO campus Calama for support.

6. References

- [1] E. Tirosh, G. Shemer, and G. Markovich, "Optimizing cobalt ferrite nanocrystal synthesis using a magneto-optical probe," *Chem. Mater.* 18, 465 – 470 (2006).
- [2] H. Gu, K. Xu, Z. Yang, C. K. Chang, and B. Xu, "Synthesis and cellular uptake of porphyrin decorated iron oxide nanoparticles-a potential candidate for bimodal anticancer therapy," *Chem. Commun.* 34, 4270-4272 (2005).
- [3] P. C. Morais, E. C. O. Lima, "Técnicas de preparação de nanopartículas magnéticas e fluidos magnéticos," In: N. Duran, L. H. C. Mattoso, and P. C. Morais, (Org). "Nanotecnologia: Introdução, preparação e caracterização de nanomateriais e exemplos de aplicação," 1 ed. São Paulo: artliber, 1, 83 (2006).
- [4] G. Baldi, D. Bonacchi, C. Innocenti, G. Lorenzi, and C. Sangregorio, "Cobalt ferrite nanoparticles: The control of the particle size and surface state and their effects on magnetic properties," *J. Magn. Magn. Mater.* 311, 10-16 (2007).
- [5] U. Luders, A. Barthelemy, M. Bibes, K. Bouzouane, S. Fusil, E. Jacquet, J. P. Contour, J. F. Bobo, J. Fontcuberta, and A. Fert, "NiFe₂O₄: A versatile spinel material brings new opportunities for spintronics," *Adv. Mater.* 18, 1733-1736 (2006).
- [6] B. Payet, D. Vincent, L. Delaunay, G. Noyel, "Influence of particle size distribution on the initial susceptibility of magnetic fluids in the Brown relaxation range" *J. Magn. Magn. Mater.* vol. 186, pp. 168-174, Jul. 1998.
- [7] C. R. Stein, M. T. S. Bezerra, G. H. A. Holanda, J. André-Filho, and P. C. Morais, "Structural and magnetic properties of cobalt ferrite nanoparticles synthesized by co-precipitation at increasing temperatures," *AIP Adv.* 8, pp. 056303 (1-8) 2017.
- [8] Z. Iatridi, K. Vamvakidis, I. Tsougos, K. Vassiou, C. Dendrinou-Samara, and G. Bokias, "Multifunctional Polymeric Platform of Magnetic Ferrite Colloidal Superparticles for Luminescence, Imaging, and Hyperthermia Applications," *ACS Appl. Mater. Interfaces*, 8, pp. 35059–35070, 2016.
- [9] A. Rossato, L. S. Silveira, P. S. Oliveira, T. T. Souza, A. P. Becker, R. Wagner, B. Kein, W. P. Souza Filho, R. C. V. Santos, D. Souza, M. D. Baldissera, M. R. Sagrillo, "Safety profile, antimicrobial and antibiofilm activities of a nanostructured lipid carrier containing oil and butter from *Astrocaryum vulgare*: in vitro studies" *International Journal for Innovation Education and Research*.9(5), 478-497 (2021).
- [10] B. M. Lacava, R. B. Azevedo, L. P. Silva, Z. G. M. Lacava, K. Skeff Neto, N. Buske, A. F. Bakuzis, and P. C. Morais, "Particle sizing of magnetite-based magnetic fluid using atomic force microscopy: A comparative study with electron microscopy and birefringence," *Appl. Phys. Lett.* 77 1876-1878 (2000).
- [11] S. Zhang, D. Dong, Y. Sui, Z. Liu, H. Wang, Z. Qian, and W. Su, "Preparation of core shell particles consisting of cobalt ferrite and silica by sol-gel process," *J. Alloy. Comp.* 415 257-260 (2006).
- [12] E. Tirosh, G. Shemer, and G. Markovich, "Optimizing cobalt ferrite nanocrystal synthesis using a

magneto-optical probe,” *Chem. Mater.* 18 465-470 (2006).

[13] K. V. P. M. Shafi, A. Gedanken, R. Prozorov, and J. Balogh, “Sonochemical preparation and size-dependent properties of nanostructured CoFe₂O₄ particles” *Chem. Mater.* 10 3445 – 3450 (1998).

[14] Q. Fanyao and P. C. Morais, “An oxide semiconductor nanoparticle in an aqueous medium: A surface charge density investigation,” *J. Phys. Chem.* 104 5232-5237 (2000).

[15] M. Rejandra, R. C. Pullar, A. K. Bhattacharya, D. Das, S. N. Chintalapudi, and C. K. Majumdar, “Magnetic properties of nanocrystalline CoFe₂O₄ powders prepared at room temperature: variation with crystallite size,” *J. Magn. Magn. Mater.* 232 71 – 83 (2001).

[16] J. F. Friedrich, J. T. Santos, A. R. Pohl, V. S. K. Nishihira, M. Brondani, J. D. Lara, I. D. Franceschi, L. R. Feksa, R. P. Raffin, “Nanocapsules with naringin and naringenin affect hepatic and renal energy metabolism without altering serum markers of toxicity in rats” *International Journal for Innovation Education and Research.* 8(10), 250-262 (2020).

[17] N. Moumen, and M. P. Pileni, “New Syntheses of cobalt ferrite particles in the range 2 – 5 nm: Comparison of the magnetic properties of the nanosized particles in dispersed fluid or in powder form,” *Chem. Mater.* 8, 1128 – 1134 (1996).

[18] Y. Li, and C. W. Park, “Particle size distribution in the synthesis of nanoparticles using microemulsions,” *Langmuir*, 15(4), 952-956 (1999).

[19] R. Massart, “Magnetic fluid and process for obtaining them,” 4329241. US Patent (1982).

[20] C. N. Chinnasamy, M. Senoue, B. Jeyadevan, O. Perales-Perez, K. Shinoda, and K. Tohji, “Synthesis of size-controlled cobalt ferrite particles with high coercivity and squareness ratio,” *J. Coll. Inter. Scien.* 263, 80-83 (2003).

[21] V. M. Boujoreanu, and E. Segal, “On the dehydration of mixed oxides powders coprecipitated from aqueous solutions,” *Soli. Stat. Scien.* 3, 407-415 (2001).

[22] Y. Kim, D. Kim, and C. S. Lee, “Synthesis and characterization of COFE₂O₄ magnetic nanoparticles prepared by temperature-controlled coprecipitation method,” *Phys. B.* 337, 42-51 (2003).

[23] C. N. Chinnasamy, B. Jeyadevan, O. Perrales-Perez, K. Shinoda, K. Tohji, and A. Kasuya, “Growth dominant co-precipitation process to achieve high coercivity at room temperature in CoFe₂O₄ nanoparticles,” *IEEE Trans. Magn.* 38(5), 2640-2642 (2002).